Received: 15 November 2023 | Revised: 9 July 2024 | Accepted: 5 August 2024

DOI: 10.1002/yea.3977

RESEARCH ARTICLE

TechnoYeast

Yeast WILEY

Marker-free genomic editing in *Saccharomyces cerevisiae* using universal donor templates and multiplexing CRISPR-CAS9

J. H. Grissom | S. E. Moody | R. J. Chi

Department of Biological Sciences, University of North Carolina at Charlotte, Charlotte, North Carolina, USA

Correspondence
R. J. Chi, Department of Biological Sciences, University of North Carolina at Charlotte, Charlotte, NC 28223, USA.
Email: richard.chi@charlotte.edu

Funding information
National Science Foundation, Grant/Award Number: 2028519; UNC Charlotte Faculty Research Grants Program

Abstract

The budding yeast *Saccharomyces cerevisiae* is an excellent model organism for studying a variety of critical cellular processes. Traditional methods to knock in or -out at specific yeast loci utilize polymerase chain reaction-based techniques, in which marker cassettes with gene-specific homologies are integrated into the genome via homologous recombination. While simple and cost-effective, these methods are limited by marker availability when multiple edits are desired. More recently, CRISPR-Cas9 technology has introduced methods to edit the yeast genome without the need for selectable markers. Although efficient, this method is hindered by additional reagents and lengthy protocols to design and test unique guide RNAs and donor templates for each desired edit. In this study, we have combined these two approaches and have developed a highly efficient economical method to edit the yeast genome marker-free. We have designed two universal donor templates that efficiently repair commonly used selectable markers when targeted by a novel guideRNA-Cas9 designed to promoter regions in *Ashbya gossypii* found in most integration modules. Furthermore, we find our newly designed guideRNA-Cas9 successfully multiplexes when multiple markers are present. Using these new tools, we have significantly improved the cost and efficiency to generate single or multiple marker-free genetic modifications. In this study, we demonstrate the effectiveness of these new tools by marker-free ablating *PRC1*, *PEP4*, and *PRB1* vacuolar proteases typically inactivated before many biochemical and membrane-trafficking studies using budding yeast.

KEYWORDS

CRISPR-Cas9, genome editing, Longtine, selectable marker

1 | INTRODUCTION

The budding yeast *Saccharomyces cerevisiae* remains an important model organism for investigating many important cellular processes, including being used in research on the etiology and pathogenesis of many human diseases (Botstein & Fink, 1988, 2011; Mohammadi et al., 2015; Pereira et al., 2012). Due to the conservation of many yeast proteins and core cellular machinery in mammalian cells, budding yeast continues to be a powerful tool that can be used to study complex interactions on a simplified scale. Over 25 years ago, *S. cerevisiae* was the first eukaryote to have its full genome sequenced, since then polymerase chain reaction (PCR)-based protocols that incorporate both auxotrophic and drug-resistance selectable markers have been the most common avenue for genome editing in yeast (Bähler et al., 1998; Janke et al., 2004; Longtine et al., 1998; Sikorski & Hieter, 1989). These methods utilize primers that include 40–50 bp of homologous sequence up- and downstream of the target gene open reading frame (ORF) and 20–25 bp of selectable marker sequence for amplification. Subsequent PCR products then recombine into the target locus via homologous recombination (Longtine et al., 1998). These major advancements led to the creation of widely used yeast collections and gave rise to the synthetic genetic array era of genomics and high-throughput studies using budding yeast (Baryshnikova, 2010; Kuzmin et al., 2014; Tong & Boone, 2006; Vizeacoumar et al., 2010). Although these original methods significantly advanced the field, researchers were limited by the number of available markers that can be used in a single mutant strain and multiple edits to a single yeast strain increased the likelihood of "marker swapping" events, which occur when a selectable marker replaces another already in the genome from a previous edit, rather than targeting its intended locus due to the similar amplification sequences used in the primers. Methods for marker recycling were developed to overcome this limitation; however, continuous utilization has been shown to decrease correct integrations and chromosomal rearrangement in the yeast genome (Akada et al., 2006). Although new selectable markers and tags have been developed, little effort has been made to directly address these limitations.

Recently, the availability of gene ablation and modification technologies using CRISPR-Cas9 systems have become widely available and others have successfully applied this tool to budding yeast (Adli, 2018; Akhmetov et al., 2018; Lee et al., 2015; Lutz et al., 2019; Utomo et al., 2021). Thus, genome edits can now be done without the need for selectable markers. These methods target Cas9 to a unique protospacer-adjacent motif (PAM) sequence in the target gene with a "guide RNA" (gRNA) specific to the region to be edited. After recognition of the PAM sequence, Cas9 precisely cuts the target locus by creating a double-stranded break. Inclusion of a user-designed "DNA donor template" with homologous sequence integrates into the target gene locus via homologous recombination. Although this method is highly efficient, drawbacks include additional cost of reagents and lengthy protocols, to design and test multiple customizable gRNAs and repair templates for each proposed edit.

Take Away

We found primer-specific regions in common PCR-based gene-editing modules that can be used as universal donor repair templates for multiple marker-free gene edits when paired with our engineered gRNA-Cas9 plasmids.

To ameliorate the cost and time-consuming design efforts required for incorporating CRISPR-Cas9 into standard yeast-editing protocols, we focused our efforts to improve existing tools. First, we found primer-specific regions in common PCR-based gene deletion modules, first described by Longtine et al. (1998), can be used as universal donor repair templates for marker-free gene editing when Cas9 is targeted to these selectable markers. Second, we engineered a gRNA-Cas9 (pJG02) that targets the *Ashbya gossypii* promoter region found in pFA6a-MX6 plasmids, which allowed for triple marker-loss in a single transformation. Third, we found common regions of the BY4741/4742 deletion collection can also be efficiently used as universal repair templates in these collections. We also found that our engineered CRISPR-Cas9 plasmid (pJG01) containing gRNA specific to His3MX6 worked more efficiently with the universal donor repair templates and allowed for sequential gene edits, thereby bypassing all marker limitations. As a proof of concept, we engineered a marker-free TVY614, a widely utilized yeast strain that contains mutations in vacuolar proteases *PRC1*, *PEP4*, and *PRB1* but has limited usage because of selectable marker availability (Giaever & Nislow, 2014; Giaever et al., 2002; Vida & Emr, 1995). Taken together, we believe our findings result in a significant improvement in PCR-based gene modifications in yeast and have pending applications to the yeast research and educational communities.

2 | MATERIALS AND METHODS

2.1 | Yeast strains, growth conditions, and transformations

All yeast strains were grown at 30°C in yeast extract-peptone-dextrose medium, unless otherwise noted. All yeast transformations were performed using the lithium acetate method (Gietz et al., 1995). For CRISPR-Cas9 transformations, carrier single-stranded DNA, Cas9 expression plasmid (250 ng), and donor DNA templates (10 µg) were added to cells and incubated for 30 min at 30°C before heat shock. Cells were grown in standard synthetic complete medium lacking nutrients required to maintain selection for auxotrophic markers and/or plasmid, unless indicated otherwise (1991). Yeast strains were constructed in BY4741/2 (*MATa/α his3-1*, *leu2-0*, *met15-0*, and *ura3-0*) by homologous recombination of gene-targeted, PCR-generated DNAs using the method of Longtine et al. (1998) and/or derived from the EUROSCARF KanMX deletion collection (Open Biosystems/Thermo Scientific) or produced by replacement of the complete reading frame with the *URA3* cassette.

Gene deletions were confirmed by PCR amplification of the deleted locus. To induce iron starvation, cells were grown to log phase in synthetic media containing 50 μM of bathophenanthrolinedisulfonic acid. Subsequent iron shock was performed by rinsing the cells with water and with synthetic media before final resuspension in synthetic media containing 500 μM Fe (III) ammonium sulfate for 2 h at 30°C as previously described (Strochlic et al., 2007, 2008).

2.2 | Immunoblotting

For quantitative immunoblot analysis of GFP-Snc1 or Ftr1-2xGFP, cells were grown under standard vegetative or iron starvation conditions to $OD_{600} \approx 0.5$, as described above. Typically, 3.0×10^7 cells were harvested by centrifugation and lysed by glass bead agitation in sodium dodecyl-sulfate polyacrylamide gel electrophoresis sample buffer. Ten percent polyacrylamide gels were loaded with 5.0×10^7 cell equivalents and transferred onto standard 0.45 μm nitrocellulose. Anti-green fluorescent protein (GFP) primary mouse monoclonal antibody (1814460, Roche) was diluted 1:2500 and Santa Cruz (sc-2055) goat antimouse horseradish peroxidase-conjugated antibody was used at 1:10,000. Anti-Pgk1 at 1:5000 (Life Technologies) was used as loading controls. Centromeric GFP-Snc1 (Shintani et al., 2002) plasmid was used in the processing assays. All enhanced chemiluminescence blots were developed on a Chemidoc-MP (Bio-Rad) and band intensities were quantified using Quantity One 1D analysis software (Bio-Rad)

2.3 | Plasmids

All CRISPR-Cas9 plasmids were constructed using the MoClo Yeast Toolkit and cloned using GoldenGate assembly (Baryshnikova, 2010). Briefly, each plasmid was constructed using three intermediates: a gRNA intermediate, a Cas9 intermediate, and a "multigene" backbone. Custom short guideRNA (sgRNA) sequences specific for either the *A. gossypii* promoter region of MX6 markers or His3MX6 were cloned into pYTK_50 entry vectors containing GFP dropout regions. Subsequent entry vectors were used to construct the sgRNA intermediate plasmid in pYTK_95.

The Cas9 intermediate were obtained from Cas9 derived from pYTK_36 and cloned into the pYTK_95 backbones. The "multigene backbone" was constructed to contain appropriate connecter sequences for final assembly, a GFP dropout region, a URA3 selectable marker, a KanR selectable marker, and a 2μ origin of replication. All three intermediates were recombined via GoldenGate assembly to produce the final Cas9 expression plasmids: pJG01 (His3MX6) and pJG02 (ALL-MX6) (Table 1).

TABLE 1 Plasmids used in this study.

Name	Plasmid marker	Source
pJG01 (HIS3MX6 specific)	Kanamycin/URA3	This Study
pJG02 (ALL-MX6)	Kanamycin/URA3	This Study
pRS315 GFP-SNC1	Ampicillin/LEU2	Lewis et al. (2000)

2.4 | Donor DNA templates and transformation efficiency

Oligonucleotides for F1-R1and U2-D2 donor DNA templates described in Table 2 were commercially synthesized and purchased from Eurofins Genomics. For F1-ADE2-R1 and U2-ADE2-D2 donor DNA templates, full-length *ADE2* was PCR amplified from genomic DNA with overhangs containing F1 and R1, or U2 and D2 sequences, respectively.

To calculate transformation efficiency, red *ade2* mutants were transformed with pJG01 or pJG02 and with associated donor DNA templates. Transformants were grown on selective media containing low 15 mg/L adenine. Candidates were scored by the presence of red or white coloration. White colonies were inferred to have successfully been edited by CRISPR-Cas9 and 10 candidates were randomly selected for PCR amplification of the deleted locus to confirm correct genomic integration sites.

2.5 | Light microscopy and image analysis

Yeast cells from cultures grown to $OD_{600} \approx 0.5$ were mounted in growth medium and three-dimensional image stacks were collected at 0.3 μm *z* increments on a DeltaVision elite workstation (Cytiva) based on an inverted microscope (IX-70; Olympus) using a ×100, 1.4 numerical aperture oil-immersion lens. Images were captured at 24°C with a 12 bit charge-coupled device camera (CoolSnap HQ; Photometrics) and deconvolved using the iterative-constrained algorithm and the measured point spread function. Image analysis and preparation was done using Softworx 6.5 (Cytiva) and ImageJ v1.50d (Rasband). To quantify vacuolar lumen localization, wild-type cells or mutants were visually scored for presence of GFP in the vacuolar lumen. GFP-Snc1 and Ftr1-2xGFP vacuolar fluorescence intensities were quantified from z stacks collected at 0.3 μm intervals. A minimum of 100 cells were used in all experimental conditions and performed in biological triplicate.

3 | RESULTS

3.1 | Marker-free strategy and efficiency

In our study, we demonstrate a significant improvement to existing yeast gene editing tools that utilize PCR-based integrations and CRISPR-Cas9 methodologies. We have found three strategies that are economical and can efficiently generate marker-free gene edits. Our first workflow requires two steps. First, the gene ORF of interest is modified using traditional PCR-based integration techniques with selectable markers (His3MX6, KanMX6, HpHMX6) as first described by Longtine et al. (1998), which results in the integration of the selectable marker flanked by F1 up- and R1 downstream sequences. Second, we use optimized gRNAs to target Cas9 to *A.*

TABLE 2 Oligos used in this study.

Name	Sequence (5′–3′)
F1-R1 Donor	CGGATCCCCGGGTTAATTAAGGCGCGCCAGATCTGTTTAGGATACTAACGCCGCCATCCAGTTTAAACGAGCTCGAATTC
U2-D2 Donor	CGTACGCTGCAGGTCGACGGATCCCCGGGTTAATTAAGGCGCCGCCATCCAGTGTCGAAAACGAGCTCGAATTCATCGAT
PRC1-F1	ACTCACTAGAGATTGTTTCTTTTCTACTCAACTTAAAGTATACATACGCTCGGATCCCCGGGTTAATTAA
PRC1-R1	TATATTTCGATCGTAGCTGATAATAAAAACGGTATGCCTACACATACACGCTGAATTCGAGCTCGTTTAAAC
PRC1-Seq F	GGGTCTCAAAGAAGGGGCCCACTAATAAAAGC
PRC1- Seq R	GAAGCAGCTCTATTGTTTTCTTTTTTTTTAATG
PEP4-F1	AGTGACCTAGTATTTAATCCAAATAAAATTCAAACAAAAACCAAAACTAACCGGATCCCCGGGTTAATTAA
PEP4-R1	CTCTCTAGATGGCAGAAAAGGATAGGGCGGAGAAGTAAGAAAAGTTTAGCGAATTCGAGCTCGTTTAAAC
PEP4-Seq F	CCTCAATTGTATTTGCTGAGGTC
PEP4-Seq R	TGATCGTACAGAGGGCGATTG
PRB1-F1	AGCTTCATCGCCAATAAAAAAACAAACTAAACCTAATTCTAACAAGCAAAGCGGATCCCCGGGTTAATTAA
PRB1-R1	CTAAGGAAAGAAAAAGAAAAAAAAAAGCAGCTGAAATTTTTCTAAATGAAGAAGAATTCGAGCTCGTTTAAAC
PRB1-Seq F	GGGCTTTCGGCTTTGGAAATTTAGGTGACTT
PRB1-Seq R	TATTTCGCGTACCTAATACATCGTCACCACACAC
PRB1-Ext F	AAAACGAGGGCTGGGAAATG
PRB1-Ext R	TGAGAAGCGGGTCACAAAGG

TABLE 3 Yeast strains used in this study.

Name	Genotype	Source
BY4741	*MATa his3Δ1 leu2Δ0 lys2Δ0 ura3Δ0*	This Study
BY4742	*MATα his3Δ1 leu2Δ0 lys2Δ0 ura3Δ0*	This Study
JGY17	*MATα his3Δ1 leu2Δ0 lys2Δ0 ura3Δ0 ade2Δ::kanMX6*	Giaever and Nislow (2014)
JGY20	*MATα ade2Δ::His3MX6 leu2Δ0 lys2Δ0 ura3Δ0*	This Study
JGY21	*MATα his3Δ1 leu2Δ0 lys2Δ0 ura3Δ0 ade2Δ*	This Study
JGY26	*MATa bar1Δ::kanMX6 tlg2Δ::His3MX6 leu2Δ0 lys2Δ0 ura3Δ0*	This Study
JGY28	*MATa his3Δ1 leu2Δ0 lys2Δ0 ura3Δ0 ade2Δ*	This Study
JGY61	*MATα his3Δ1 leu2Δ0 lys2Δ0 ura3Δ0 prb1Δ::kanMX6*	Giaever and Nislow (2014)
JGY63	*MATα* FTR1-2xGFP::HIS3 *leu2Δ0 lys2Δ0 ura3Δ0*	This Study
JGY64	*MATα* FTR1-2xGFP::HIS3 *leu2Δ0 lys2Δ0 ura3Δ0 prc1Δ pep4Δ prb1Δ*	This Study
JGY71	*MATa prc1Δ::hphMX6 his3Δ1 leu2Δ0 lys2Δ0 ura3Δ0*	This Study
JGY72	*MATa bar1Δ::kanMX6 tlg2Δ::His3MX6 prc1Δ::hphMX6 leu2Δ0 lys2Δ0 ura3Δ0*	This Study
JGY73	*bar1Δ tlg2Δ his3Δ1 leu2Δ0 lys2Δ0 ura3Δ0*	This Study
JGY74	*bar1Δ tlg2Δ prc1Δ his3Δ1 leu2Δ0 lysΔ0 ura3Δ0*	This Study
JGY614	*MATα his3Δ1 leu2Δ0 lys2Δ0 ura3Δ0 prc1Δ pep4Δ prb1Δ*	This Study

gossypii promoter sequences found in most pFA6a-MX6 derived integration cassettes (Figure 1a). We found our gRNA-Cas9s in pJG01 or pJG02 sufficiently created double-stranded breaks, which promotes efficient replacement of the selectable marker by a single stranded 80 bp concatenated F1-R1 donor oligo (Table 2) via homologous recombination. Similarly, we found the KanMX6 selectable marker in the commercially available BY4742 deletion collection were also flanked by U2 up- and D2 downstream sequences

TABLE 4 Primers used to confirm JGY614.

Name	Sequence (′5–3′)	Expected size	
P1	GGGTCTCAAAGAAGGGGCCCACTAATAAAAGC	Full length:	2021 bp
P2	GAAGCAGCTCTATTGTTTTCTTTTTTTTTAATG	*His3MX6Δ:*	1825 bp
		Marker-free:	502 bp
P3	CCTCAATTGTATTTGCTGAGGTC	Full length:	2168 bp
P4	TGATCGTACAGAGGGCGATTG	*His3MX6Δ:*	2353 bp
		Marker-free:	1030 bp
P5	GGGCTTTCGGCTTTGGAAATTTAGGTGACTT	Full length:	2472 bp
P6	TATTTCGCGTACCTAATACATCGTCACCACACAC	*His3MX6Δ:*	2125 bp
		Marker-free:	646 bp
P7	ACTCACTAGAGATTGTTTCTTTTCTACTCAACTTAAAGTATACATACGCTCGGATCCCCGGGTTAATTAA	His3MX6:	1403 bp
P8	TATATTTCGATCGTAGCTGATAATAAAAACGGTATGCCTACACATACACG CTGAATTCGAGCTCGTTTAAAC		
P9	AGTGACCTAGTATTTAATCCAAATAAAATTCAAACAAAAACCAAAACTAACCGGATCCCCGGGTTAATTAA	His3MX6:	1403 bp
P10	CTCTCTAGATGGCAGAAAAGGATAGGGCGGAGAAGTAAGAAAAGTTTAGCGAATTCGAGCTCGTTTAAAC		
P11	AAAACGAGGGCTGGGAAATG	*prb1Δ::kanMX6:*	2251 bp
P12	TGAGAAGCGGGTCACAAAGG		

at the sites of integration which can also be targeted by pJG02 and replaced using a single stranded 80 bp concatenated U2-D2 Donor oligo (Table 2) via homologous recombination to produce marker-free genomic modifications (Giaever & Nislow, 2014).

To measure the efficiency of our marker-free strategy, we utilized a red to white screen using *ade2* mutants that accumulate purine precursors in the Ade2 biosynthesis pathway, which can easily be visualized as red phenotype on low adenine media (15 mg/L) (Gedvilaite & Sasnauskas, 1994; Ugolini & Bruschi, 1996). We applied our marker-free strategy on *ade2* mutants derived from PCR-based knockouts containing His3MX6, KanMX6, HphMX6, or an *ade2Δ*::kanMX6 obtained from the BY4742 deletion collection (Figure 1). To determine the efficiency of our strategy, we modified the DNA donor templates to include a wild-type copy of the *ADE2* gene within each donor template. We found successful replacement of the selectable markers with the ADE2 donor DNA template resulted in the cells restoring ADE2 biosynthesis, which ameliorated the red phenotype and returned the cells to white when grown on low adenine media. Using this assay, we determined our F1-R1 donor DNA template exhibited a high degree of efficiency for His3MX6, KanMX6, and HphMX6 with 85%, 90%, and 90% reverting to white, respectively (Figure 2). Although the U2-D2 DNA donor repair template was far less efficient, with only 35% of colonies reverting to white (Figure 2).

3.2 | Creation of a marker-free protease-deficient strain

Next, we sought to determine if the integrated donor DNA templates would prohibit subsequent modifications using repeated marker-free ablations. To test this, we narrowed our focus to generating a useful tool for the yeast research community and decided to apply our strategy by engineering a marker-free protease-deficient yeast strain. We found inspiration using TVY614, a well-utilized protease-deficient yeast strain commonly used for studying protein overexpression and membrane trafficking first developed by the Emr Lab (Vida & Emr, 1995). In this strain, three major vacuolar proteases Pep4, Prc1, and Prb1 were knocked out using classical yeast genetic manipulations using selectable markers. Although the TVY614 strain has been an excellent asset to many research labs for the past 30 years, the strain's limited available selectable markers have long restricted most experiments to just a few genetic modifications. Therefore, we believed a marker-free variant of this strain would be a desirable reagent to the yeast community and successfully engineered the strain using the following steps.

In sequential order, we first deleted *PRC1* with standard PCR-based genomic editing using His3MX6 flanked by F1 and R1 sequences (Figure 3d, Lane 4). Next, we transformed these cells with pJG01, the gRNA-Cas9 specific to HisMX6 and the F1-R1 DNA donor template (Figure 3a). All candidates were PCR verified and grown on 5-FOA to drop out the gRNA-Cas9 plasmid (Table 4). The procedure was repeated for *PEP4* marker-free deletion without incident (Figure 3b). However, upon repeating the procedure for a third time for the *PRB1* locus, we failed to insert a PCR amplified His3MX6 cassette into the gene locus, suggesting multiple F1-R1 sequences in the genome negatively affected subsequent modifications, likely causing nonspecific marker integrations. However, we did eventually find success by amplifying genomic DNA 350 bp up and downstream from the *prb1Δ::kanMX6* locus obtained from the BY4742 deletion collection (Figure 3c). We hypothesized the larger

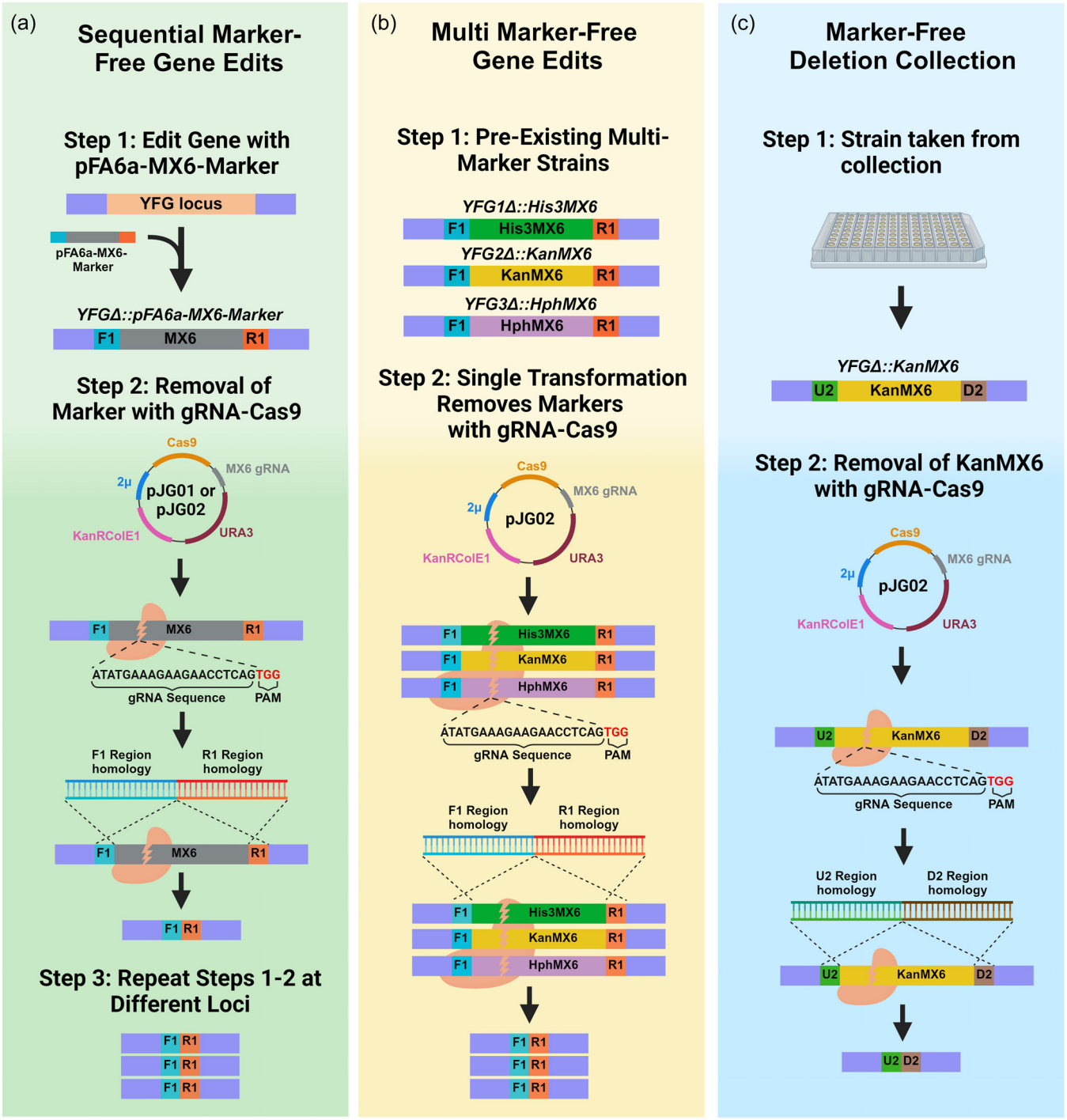

FIGURE 1 Marker-free genomic editing. Our method uses a combination of traditional gene manipulation techniques using polymerase chain reaction (PCR)-based selectable markers followed by removal using CRISPR-Cas9. (a) Genes modified using the traditional Longtine et al. (1998) technique have residual F1 and R1 sequences located up- and downstream of the selectable marker. Transformation with CRISPR plasmid pJG01 or pJG02 and the F1-R1 donor repair template results in the removal of the selectable marker. Steps may be sequentially repeated to generate multimarker-free gene edits. (b) The guide RNA (gRNA) of pJG02 targets the *Ashbya gossypii* promoter region found in all pFA6a-MX6 cassettes, allowing for multiplexed removal of markers. Transformation of pJG02 and the F1-R1 donor repair template into a yeast strain harboring multiple MX6-based gene deletions results in simultaneous removal of all MX6 markers. (c) BY4741/2 deletion collections have residual U2 and D2 sequences located up- and downstream of the KanMX6 selectable marker. Transformation with CRISPR plasmid (pJG02) and the U2-D2 donor repair template results in the removal of the selectable marker.

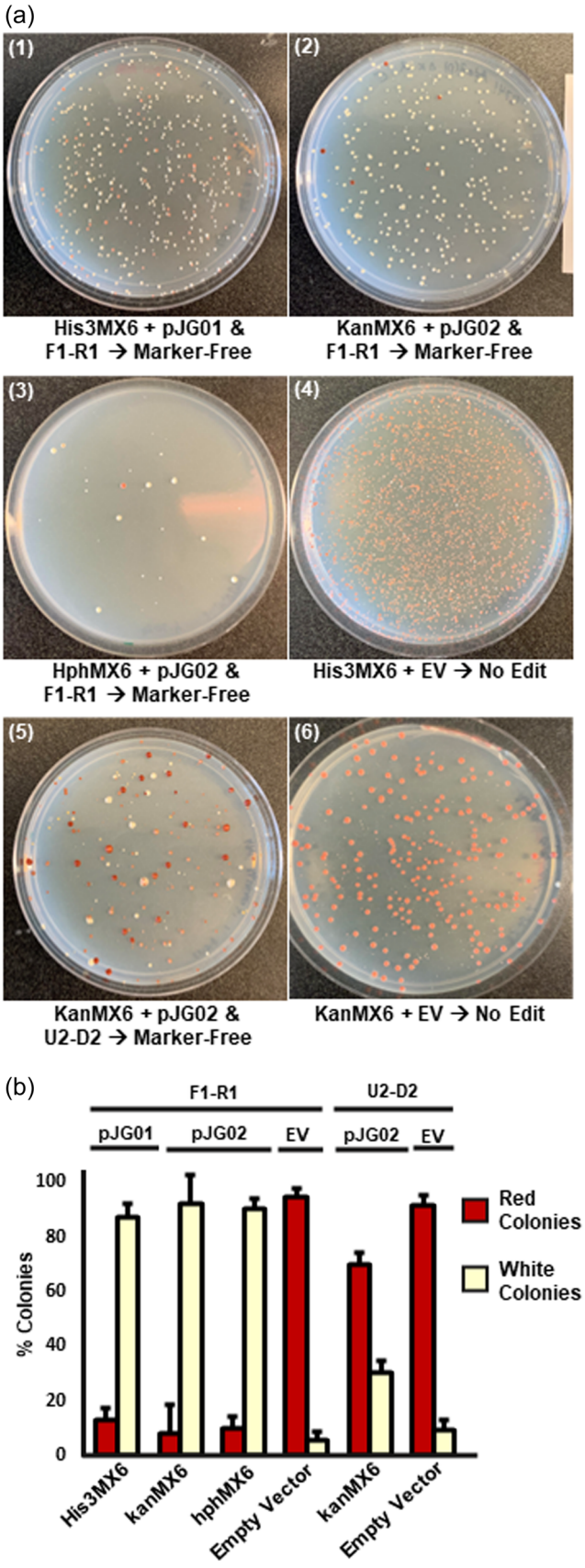

amount of homologous sequence combined with the absence of F1-R1 sequence would drive greater specificity during homologous recombination. Indeed, using this strategy we obtained >100 isolates of *prc1Δ pep4Δ prb1Δ::kanMX6*, which was then targeted for marker removal using pJG02 in conjunction with the U2-D2 donor DNA template (Figure 3c). We also found the final selectable marker removal via gRNA-Cas9 was highly efficient and resulted in >100 candidates of which four isolates were confirmed by PCR. We have named the resulting strain JGY614 to acknowledge the clear emulation to the original TVY614 strain and is available upon request (Figure 3e).

To confirm vacuole proteostasis is impaired in JGY614, we visualized and measured the steady state protein abundance of two well-characterized vacuolar localizing proteins, Snc1 and Ftr1. Snc1 is a v-SNARE that has been shown to traffic to the vacuole through multiple pathways, and Ftr1, an iron transporter that is primarily found on the plasma membrane and is trafficked to the vacuole for degradation upon binding to iron complexes (Grissom et al., 2020; Ma & Burd, 2019; Ma et al., 2017; Strochlic et al., 2007, 2008). In JGY614, GFP-Snc1 showed clear retention at the plasma membrane and a strong vacuole signal as compared to wild-type cells (Figure 4a). Recently, sorting nexin Snx4 was found to mediate Snc1 trafficking from the vacuole membrane, resulting in increased Snc1 degradation in *snx4Δ* cells (Ma et al., 2017). Here we confirm these results; however, when Snx4 is ablated in JGY614, cells exhibited far less vacuole fluorescence intensities and contained many internal compartments, indicating multiple trafficking defects are present (Figure 4a). Quantitative immunoblot analysis of steady-state GFP-Snc1 further confirmed the loss of Snc1 degradation in JGY614. GFP-Snc1 was found to be 30% degraded in wild-type cells and 40%

FIGURE 2 Marker-free transformation efficiency.
(a) Representative images of transformation C-URA plates following indicated selectable marker removal using pJG01 or pJG02 with donor repair templates. Plates 1–3 represent His3MX6, KanMX6, and HphMX6 repaired with F1-ADE2-R1 donor template, respectively, using pJG01 and pJG02. Plate 5 represents *ade2Δ*::kanMX6 from the BY4742 deletion collection repaired with U2-ADE2-D2 donor template using pJG02. Plates 4 and 6 represent transformations of *ade2Δ*::HisMX6 or *ade2Δ*::kanMX6 using empty vectors with their indicated donor repair templates, respectively. (b) Transformation efficiency was calculated by the ratio of pink/red to white colonies. F1-ADE2-R1 donor efficiency when targeting HisMX6, KanMX6, and HphMX6 was 85%, 90%, and 90%, respectively. Transformation efficiency was reduced to 35% when using U2-ADE2-R1 donor repair template in *ade2Δ*::kanMX6 obtained the BY4742 deletion collection. Additionally, each *ade2Δ* strain transformed with empty vector show 5% and 10% reversion to white colonies, respectively. Results were calculated from three biological replicates. Ratio of red and white colonies from total colonies on each plate are reported with error bars representing 1 SD of the mean.

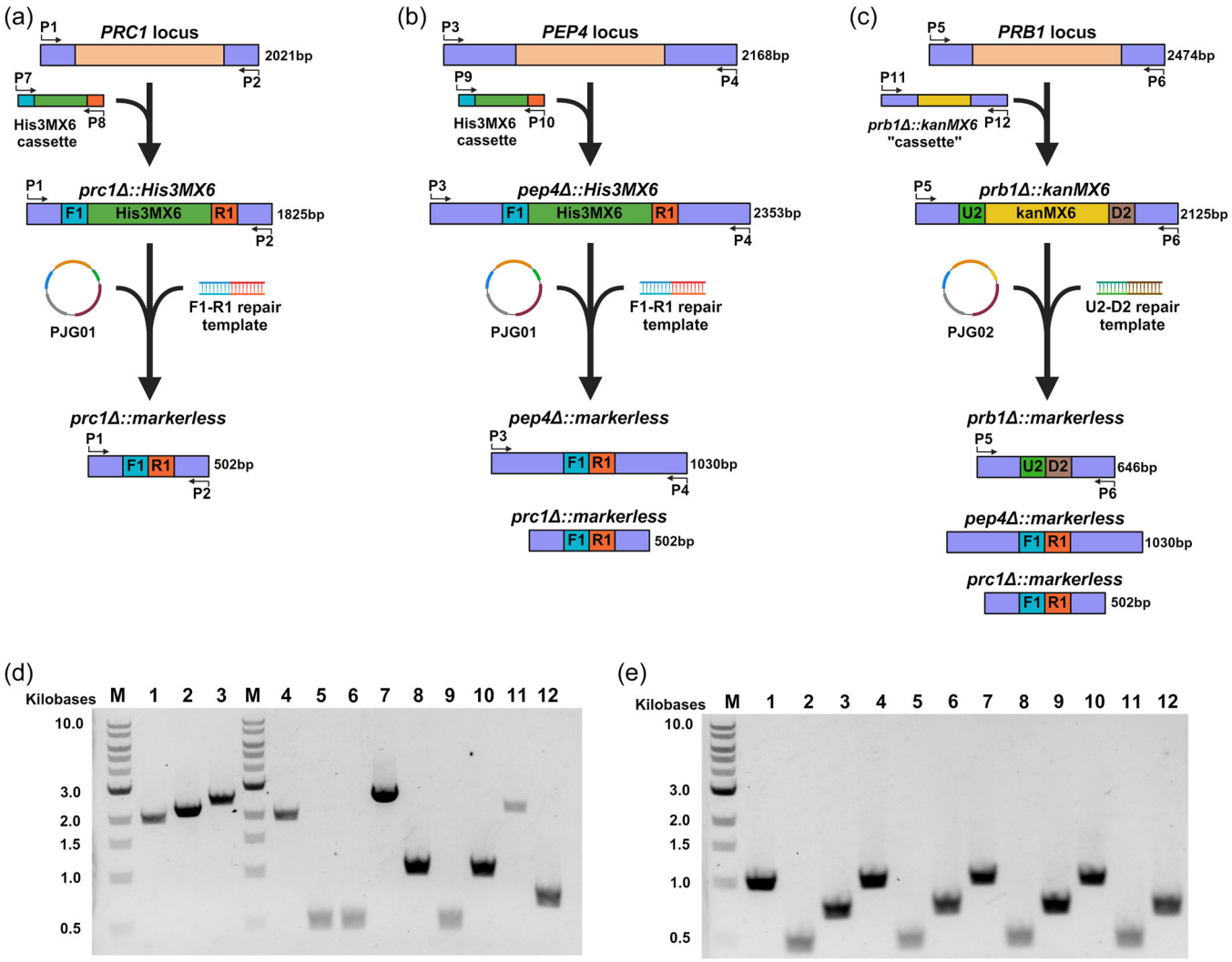

FIGURE 3 Engineering a marker-free protease deficient strain using sequential marker-free knockouts. (a–c) Vacuolar proteases, Prc1, Pep4, and Prb1 were sequentially targeted for marker-free deletion. PRC1 was knocked out first using standard polymerase chain reaction (PCR)-based marker techniques, and His3MX6 marker was removed by Cas9 and replaced by the F1-R1 donor repair template. This was followed by Pep4 and then Prb1 sequentially using a similar approach, except KanMX6 was used for Prb1. (d) PCR using indicated primers (Table 3) on genomic DNA was used at each step to confirm each successful genomic integration. Lanes 1–3 bands demonstrate the presence of PRC1, PEP4, and PRB1, respectively, in our beginning strain. Lane 4 indicates the successful replacement of PRC1 with HisMX6, followed by the removal of the marker by Cas9 as shown in lanes 5–6. Lane 7 indicates the successful replacement of PEP4 with His3MX6, followed by the removal of the marker by Cas9, as shown in lanes 8 and 10, while maintaining the PRC1 locus marker-free shown in lane 9. Lane 11 indicates the successful replacement of PRB1 with KanMX6, followed by the removal of the marker by Cas9 as shown in lanes 12. (e) Final genotypes of four marker-free isolates of TGY614 *MATα his3Δ1 leu2Δ0 lys2Δ0 ura3Δ0 prc1Δ pep4Δ prb1Δ* were confirmed at the PRC1 locus (lanes 1, 4, 7, 10), PEP4 locus (lanes 2, 5, 8, 11), and PRB1 locus (lanes 3, 6, 9, 12). All primers and expected sizes are described in Table 4.

degraded in *snx4D* cells. In JGY614, GFP-Snc1 degradation is reduced to 9% in wild-type and 5% in JGY614 (Figure 4b). Similarly, we localized Ftr1-2xGFP under iron replete conditions which causes rapid processing of Ftr1 as it is trafficked to the vacuole for degradation. After 2 h in iron replete conditions, Ftr1-2xGFP was retained in the vacuole and plasma membrane in JGY614, while very little fluorescence was present in wild-type cells (Figure 4c). Quantitative immunoblot analysis of steady-state Ftr1-2xGFP found protein abundance was increased 10-fold in JGY614 as compared to wild-type cells, indicating vacuolar proteases are greatly impaired (Figure 4d).

3.3 | Marker-free gene deletions using multiplexing Cas9

Next, as pJG02 targets *A. gossypii* promoter sequences found in most pFA6a-MX6-derived integration cassettes, we hypothesized that the gRNA-Cas9 would multiplex to remove multiple selectable markers in a single transformation, thereby significantly reducing the time and efforts to create multiple marker-free gene deletions. To test for this, we transformed pJG02 and the F1-R1 donor repair template into JGY26, a strain with KanMX6 and HisMX6 integrated to ablate *BAR1* and *TLG2* loci, respectively. We found marker removal efficiency was

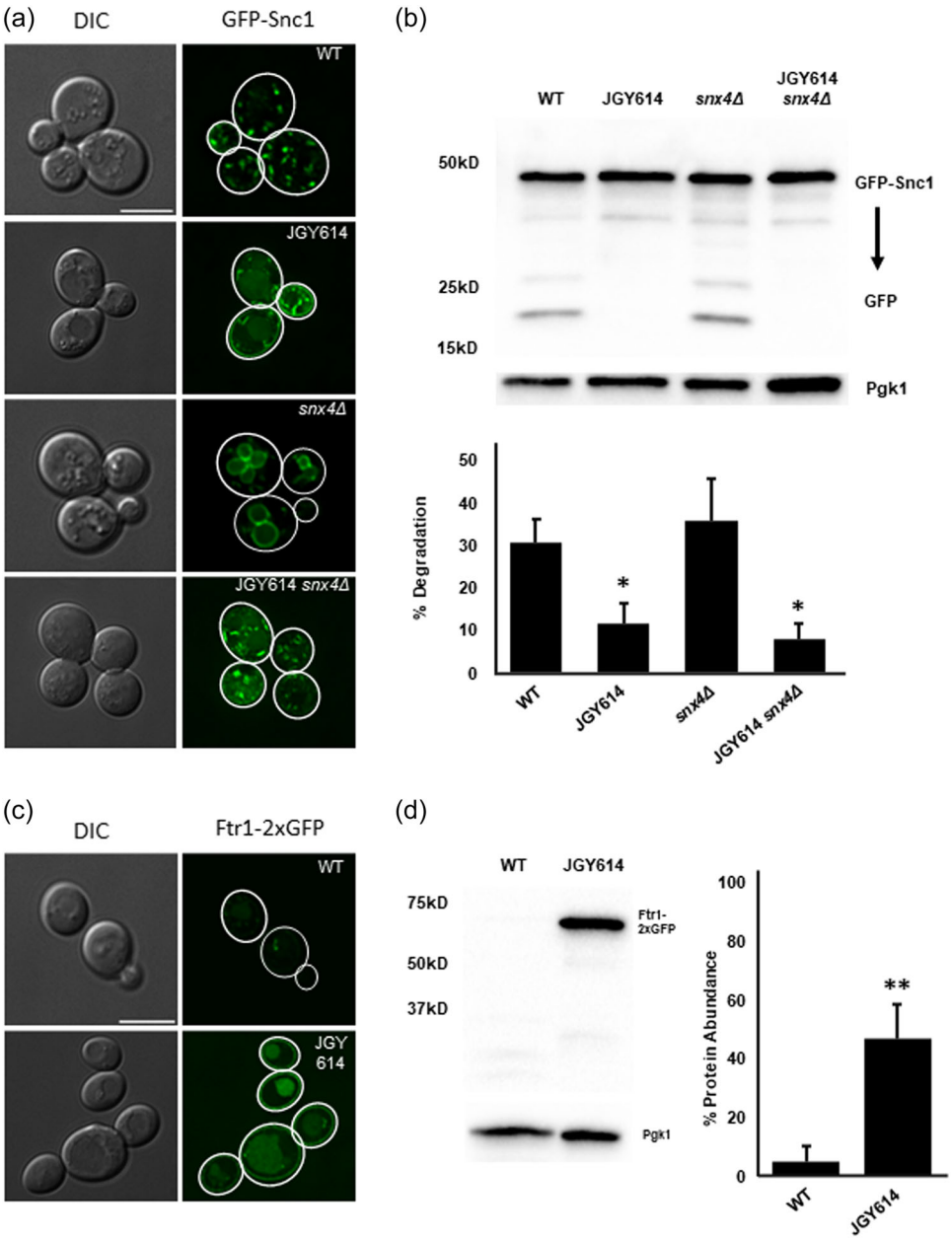

FIGURE 4 JGY614 vacuole proteostasis is impaired. (a, c) Two proteins normally trafficked to the vacuole and degraded were tagged with green fluorescent protein (GFP) in wild type (WT) or JGY614 cells. (a) Micrographs indicate SNARE protein GFP-Snc1 and Ftr1-2xGFP recycles from to and from the plasma membrane via an endovacuolar pathway and both GFP signals are enriched in JGY614 backgrounds. (b) GFP-Snc1 processing assay resulted in a 30% degradation, this is exacerbated to 40% in *snx4Δ* cells. In JGY614, GFP-Snc1 degradation is reduced to 9% and 5%, respectively. Graph values were analyzed via single-factor analysis of variance and Tukey honest significance test, with asterisks (*) representing $p < 0.05$. (d) Ftr1-GFP processing assay after WT and JGY-614 were replete of iron. In WT cells, Ftr1-GFP is nearly undetectable by western blot analysis but stabilized in JGY614 cells. Values were analyzed via unpaired *T* test, with asterisks (**) representing $p < 0.01$. All scale bars indicate 5 µm. In the graphs in b and d, results were calculated from three biological replicates and error bars represent 1 SD of the mean.

reduced to ~45% as compared to 95% when one selectable marker was present (Figure 5a,b). Similarly, when three selectable markers are present as in JGY72, a strain with KanMX6, His3MX, and HphMX6, integrated to ablate *BAR1*, *TLG2*, and *PRC1* loci, respectively. We found marker removal efficiency slightly reduced to ~40% as compared to the 1X or 2X transformations (Figure 5a–c). Surprisingly, we found for all multimarker removal experiments, all transformation colonies were either completely ablated of each marker, or maintained every marker, indicating multiplexing Cas9 did not preferentially target a specific selectable marker but when successful, targeted at 100% efficacy. Therefore, using this strategy yeast strains with three or more pre-existing selectable markers derived from pFA6a-MX6 integration cassettes, would only require a single transformation reaction to create a multigene marker-free yeast strain.

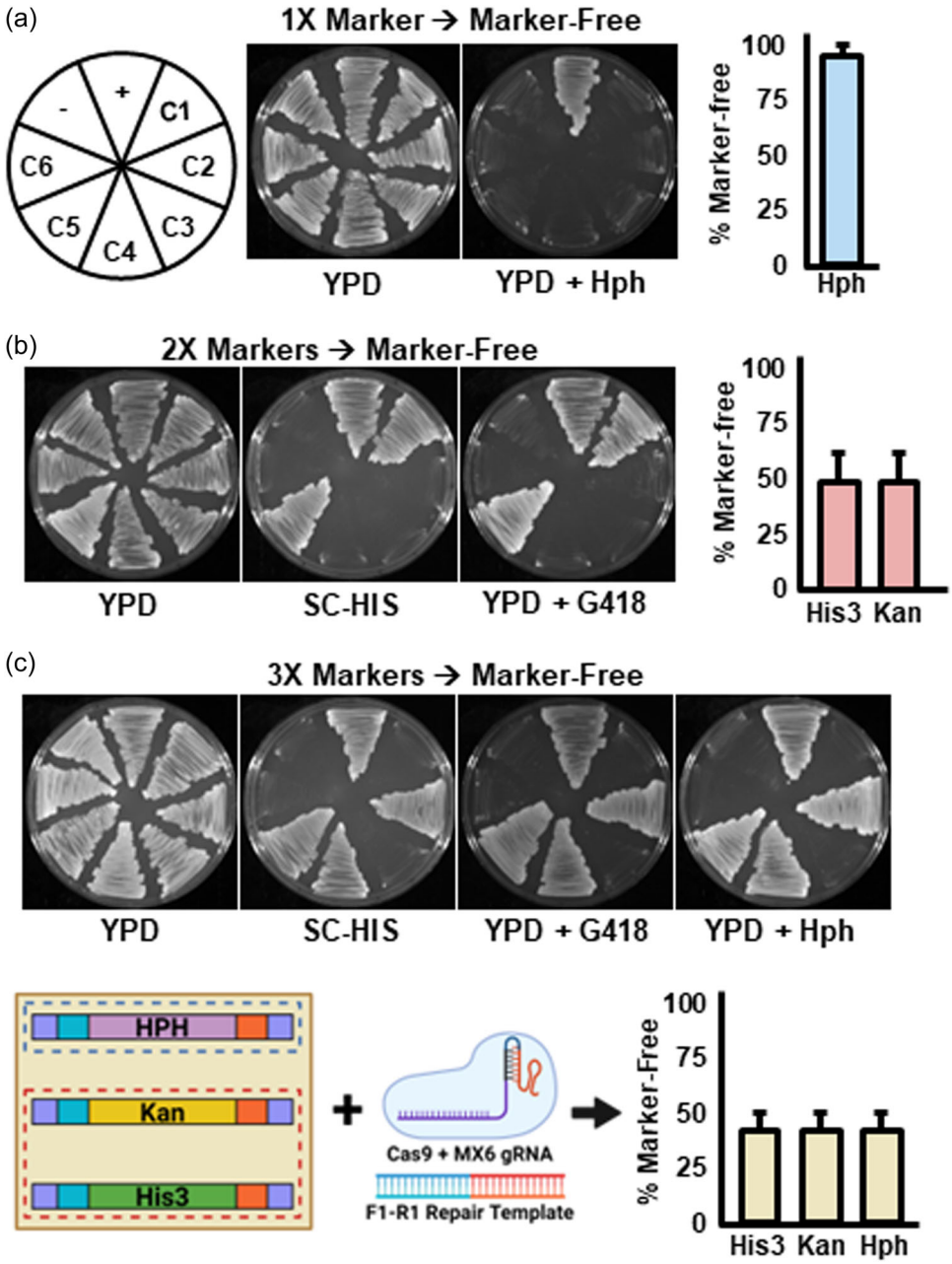

FIGURE 5 Multiplexing CRISPR-Cas9 efficiency. Plates shown in a–c represent transformation efficiency when 1X, 2X, or 3X markers are present and transformed with pJG02 and the F1-R1 donor repair template, respectively. (a) Plate legend for all transformation plates is shown. Each plate includes the beginning strain that corresponds to the integrated MX6 marker(s) as a positive (+) control, a negative (−) control background strain BY4741 and six random colonies from each indicated transformation reaction (C1–C6). Successful marker-free transformants no longer grew on selective media as compared to beginning strains but grew robustly on YPD plates. When a single marker (1X) HphMX6 was present, 95% of resulting transformations colonies were found to be marker-free. (b) When two markers (2X) were present (His3MX6, KanMX6), 45% of resulting transformation colonies were found to be marker-free. (c) When all three markers (3X) were present (HphMX6, His3MX6, KanMX6), 40% of resulting transformation colonies were found to be marker-free. Notably, for all multimarker experiments, all candidates were either completely ablated of each marker, or maintained every marker, indicating multiplexing CAS9 did not preferentially target a specific selectable marker. Results were calculated from three biological replicates and error bars represent 1 SD of the mean. YPD, yeast extract-peptone-dextrose.

4 | DISCUSSION

In this study, we have successfully combined traditional PCR-based techniques with CRISPR-Cas9 to create an economical and efficient strategy to edit the yeast genome marker-free. We believe this system satisfactorily addresses many of the drawbacks and limitations that may have prevented some yeast research labs from routinely adopting CRISPR-Cas9 protocols in their labs. First, we tested multiple gRNAs and have optimized two that efficiently target Cas9 to commonly used selectable markers. pJG01 specifically targets

His3MX6 and can be used for sequential multimarker deletions or when single marker deletion is preferred (Figure 3). Second, we discovered common sequences found in traditional PCR-based techniques used to modify yeast can be used as donor DNA templates to remove selectable markers in combination with associated gRNA-Cas9 constructs. Therefore, two "universal" donor DNA templates comprising of either F1 and R1 for strains derived by Longtine et al. (1998) or U2 and D2 sequences for strains derived from the BY4741/2 deletion collections are required in conjunction with the associated gRNA-Cas9 plasmids. These donor DNA templates are single stranded oligos which can be synthesized commercially at high concentrations for just a few dollars. We especially found markers knocked out using F1-R1 donor DNA templates occurred at a higher efficiency than using the U2-D2 donor DNA templates. Finally, we have demonstrated the ability to sequentially modify and remove selectable markers at least three times during the engineering of our marker-free protease-deficient strain, JGY614. In our experience, using a sequential approach; one to two marker-free modifications can occur at high frequency; however, subsequent modifications result in a significant reduction in specificity. Additionally, we suspect that as the number of marker-free modifications accumulates the chances of nonspecific recombination at previously modified loci also increases. In these cases, we suggest increasing flanking homologous sequences and alternating donor DNA templates and selectable markers, if possible. In our experience, we found sequential marker-free editing of one to two genes is generally trouble-free, while three or more edits is more challenging. Although we have successfully edited eight loci using sequential edits and have not found any true limitations to this strategy.

We have also made significant efforts to multiplex two or more gRNAs with multiple selectable markers into a single Cas9 plasmid. However, we found all our multiplexed gRNA-Cas9 plasmids were not nearly as effective as our individual constructs. Others have noted a similar reduction in efficiency and hypothesized Cas9 concentrations maybe rate limiting when split between additional gRNAs, while others have found success targeting up to four different loci with four separate gRNAs expressed on the same CRISPR-Cas9 plasmid (Lee et al., 2015). Likewise, others have previously designed gRNA-Cas9 to specifically target a sequence shared by several selectable marker cassettes; however, their method required synthesizing unique repair templates for each allelic exchange and was not applied to large scale multiple marker-free strain engineering (Lutz et al., 2019). In the current study, we also designed a gRNA-Cas9 that targets sequences found in most pFA6a series integration cassettes and found when combined with our novel universal donor templates, can multiplex and create DNA breaks at three unique loci. This is especially useful when pre-existing strains harbor multiple markers and we found it can efficiently and accurately remove multiple selectable markers in a single transformation (Figure 5), these constructs are available by request.

Taken together, we believe our findings result in a significant improvement in PCR-based gene editing methodologies in yeast. We believe our strategy can be easily applied to any yeast collection that has been derived by pFA6a-MX6 integration cassettes and has common sequences flanking the selectable markers. Additionally, our gRNA-Cas9 constructs can be used to perform an unlimited number of gene edits, therefore researchers can modify entire pathways or protein families, faster and cheaper than any other available system. Likewise, we believe this new strategy can easily be adapted as a low cost but effective educational tool to demonstrate CRISPR-Cas9 technology in the classroom.

AUTHOR CONTRIBUTIONS

James H. Grissom designed the experiments, conducted the experiments, and wrote the manuscript. Sarah E. Moody conducted the experiments and wrote initial draft of the manuscript. Richard J. Chi contributed in conceptualization of the research and wrote the manuscript.

ACKNOWLEDGMENTS

We are grateful to the members of the Chi Lab and Mandi Ma for thoughtful discussions and comments on this manuscript. We would like to thank undergraduate researchers Alyssa Lucero, Carrie Rapier, Jordan Swaby, and Briggs Yoder for their direct efforts in developing the project. This work was supported by the National Science Foundation 2028519 to R. J. Chi and UNC Charlotte Faculty Research Grants Program to R. J. Chi.

DATA AVAILABILITY STATEMENT

The data that support the findings of this study are available on request from the corresponding author. The data are not publicly available due to privacy or ethical restrictions.

ORCID

R. J. Chi http://orcid.org/0000-0003-4830-6685

REFERENCES

Adli, M. (2018). The CRISPR tool kit for genome editing and beyond. *Nature Communications*, *9*(1), 1911.

Akada, R., Kitagawa, T., Kaneko, S., Toyonaga, D., Ito, S., Kakihara, Y., Hoshida, H., Morimura, S., Kondo, A., & Kida, K. (2006). PCR-mediated seamless gene deletion and marker recycling in *Saccharomyces cerevisiae*. *Yeast*, *23*(5), 399–405.

Akhmetov, A., Laurent, J., Gollihar, J., Gardner, E., Garge, R., Ellington, A., Kachroo, A., & Marcotte, E. (2018). Single-step precision genome editing in yeast using CRISPR-Cas9. *BIO-PROTOCOL*, *8*(6), e2765.

Bähler, J., Wu, J. Q., Longtine, M. S., Shah, N. G., Mckenzie III, A., Steever, A. B., Wach, A., Philippsen, P., & Pringle, J. R. (1998). Heterologous modules for efficient and versatile PCR-based gene targeting in *Schizosaccharomyces pombe*. *Yeast*, *14*(10), 943–951.

Baryshnikova, A., et al (2010). Synthetic genetic array (SGA) analysis in *Saccharomyces cerevisiae* and *Schizosaccharomyces pombe*. *Methods in Enzymology*, *470*, 145–179.

Botstein, D., & Fink, G. R. (1988). Yeast: An experimental organism for modern biology. *Science*, *240*, 1439–1443.

Botstein, D., & Fink, G. R. (2011). Yeast: An experimental organism for 21st century biology. *Genetics*, *189*(3), 695–704.

Gedvilaite, A., & Sasnauskas, K. (1994). Control of the expression of the ADE2 gene of the yeast *Saccharomyces cerevisiae*. *Current Genetics*, *25*(6), 475–479.

Giaever, G., Chu, A. M., Ni, L., Connelly, C., Riles, L., Véronneau, S., Dow, S., Lucau-Danila, A., Anderson, K., André, B., Arkin, A. P., Astromoff, A., El Bakkoury, M., Bangham, R., Benito, R., Brachat, S., Campanaro, S., Curtiss, M., Davis, K., … Johnston, M. (2002). Functional profiling of the *Saccharomyces cerevisiae* genome. *Nature*, *418*(6896), 387–391.

Giaever, G., & Nislow, C. (2014). The yeast deletion collection: A decade of functional genomics. *Genetics*, *197*(2), 451–465.

Gietz, R. D., Schiestl, R. H., Willems, A. R., & Woods, R. A. (1995). Studies on the transformation of intact yeast cells by the LiAc/SS-DNA/PEG procedure. *Yeast*, *11*(4), 355–360.

Grissom, J. H., Segarra, V. A., & Chi, R. J. (2020). New perspectives on SNARE function in the yeast minimal endomembrane system. *Genes*, *11*(8), 899.

Janke, C., Magiera, M. M., Rathfelder, N., Taxis, C., Reber, S., Maekawa, H., Moreno-Borchart, A., Doenges, G., Schwob, E., Schiebel, E., & Knop, M. (2004). A versatile toolbox for PCR-based tagging of yeast genes: New fluorescent proteins, more markers and promoter substitution cassettes. *Yeast*, *21*(11), 947–962.

Kuzmin, E., Sharifpoor, S., Baryshnikova, A., Costanzo, M., Myers, C. L., Andrews, B. J., & Boone, C. (2014). Synthetic genetic array analysis for global mapping of genetic networks in yeast. *Methods in Molecular Biology*, *1205*, 143–168.

Lee, M. E., DeLoache, W. C., Cervantes, B., & Dueber, J. E. (2015). A highly characterized yeast toolkit for modular, multipart assembly. *ACS Synthetic Biology*, *4*(9), 975–986.

Lewis, M. J., Nichols, B. J., Prescianotto-Baschong, C., Riezman, H., & Pelham, H. R. B. (2000). Specific retrieval of the exocytic SNARE Snc1p from early yeast endosomes. *Molecular Biology of the Cell*, *11*(1), 23–38. https://doi.org/10.1091/mbc.11.1.23

Longtine, M. S., Mckenzie III, A., Demarini, D. J., Shah, N. G., Wach, A., Brachat, A., Philippsen, P., & Pringle, J. R. (1998). Additional modules for versatile and economical PCR-based gene deletion and modification in *Saccharomyces cerevisiae*. *Yeast*, *14*(10), 953–961.

Lutz, S., Brion, C., Kliebhan, M., & Albert, F. W. (2019). DNA variants affecting the expression of numerous genes in trans have diverse mechanisms of action and evolutionary histories. *PLoS Genetics*, *15*(11), e1008375.

Ma, M., & Burd, C. G. (2019). Retrograde trafficking and quality control of yeast synaptobrevin, Snc1, are conferred by its transmembrane domain. *Molecular Biology of the Cell*, *30*(14), 1729–1742.

Ma, M., Burd, C. G., & Chi, R. J. (2017). Distinct complexes of yeast Snx4 family SNX-BARs mediate retrograde trafficking of Snc1 and Atg27. *Traffic*, *18*(2), 134–144.

Mohammadi, S., Sabaridokht, B., Subramaniam, S., & Grama, A. (2015). Scope and limitations of yeast as a model organism for studying human tissue-specific pathways. *BMC Systems Biology*, *9*, 96.

Pereira, C., Bessa, C., Soares, J., Leão, M., & Saraiva, L. (2012). Contribution of yeast models to neurodegeneration research. *Journal of Biomedicine and Biotechnology*, *2012*, 1–12.

Shintani, T., Huang, W. P., Stromhaug, P. E., & Klionsky, D. J. (2002). Mechanism of cargo selection in the cytoplasm to vacuole targeting pathway. *Developmental Cell*, *3*(6), 825–837.

Sikorski, R. S., & Hieter, P. (1989). A system of shuttle vectors and yeast host strains designed for efficient manipulation of DNA in *Saccharomyces cerevisiae*. *Genetics*, *122*(1), 19–27.

Strochlic, T. I., Schmiedekamp, B. C., Lee, J., Katzmann, D. J., & Burd, C. G. (2008). Opposing activities of the Snx3-retromer complex and ESCRT proteins mediate regulated cargo sorting at a common endosome. *Molecular Biology of the Cell*, *19*(11), 4694–4706.

Strochlic, T. I., Setty, T. G., Sitaram, A., & Burd, C. G. (2007). Grd19/Snx3p functions as a cargo-specific adapter for retromer-dependent endocytic recycling. *The Journal of Cell Biology*, *177*(1), 115–125.

Tong, A. H., & Boone, C. (2006). Synthetic genetic array analysis in *Saccharomyces cerevisiae*. *Methods in Molecular Biology (Clifton, N.J.)*, *313*, 171–192.

Ugolini, S., & Bruschi, C. V. (1996). The red/white colony color assay in the yeast *Saccharomyces cerevisiae*: Epistatic growth advantage of white ade8-18, ade2 cells over red ade2 cells. *Current Genetics*, *30*(6), 485–492.

Utomo, J. C., Hodgins, C. L., & Ro, D. K. (2021). Multiplex genome editing in yeast by CRISPR/Cas9 - A potent and agile tool to reconstruct complex metabolic pathways. *Frontiers in Plant Science*, *12*, 719148.

Vida, T. A., & Emr, S. D. (1995). A new vital stain for visualizing vacuolar membrane dynamics and endocytosis in yeast. *The Journal of Cell Biology*, *128*(5), 779–792.

Vizeacoumar, F. J., van Dyk, N., S.Vizeacoumar, F., Cheung, V., Li, J., Sydorskyy, Y., Case, N., Li, Z., Datti, A., Nislow, C., Raught, B., Zhang, Z., Frey, B., Bloom, K., Boone, C., & Andrews, B. J. (2010). Integrating high-throughput genetic interaction mapping and high-content screening to explore yeast spindle morphogenesis. *Journal of Cell Biology*, *188*(1), 69–81.

How to cite this article: Grissom, J. H., Moody, S. E., & Chi, R. J. (2024). Marker-free genomic editing in *Saccharomyces cerevisiae* using universal donor templates and multiplexing CRISPR-CAS9. *Yeast*, *41*, 568–579. https://doi.org/10.1002/yea.3977